THE UNIVERSITY OF TEXAS
MD Anderson Cancer Center
Making Cancer History®

Detection of vessel bifurcations in 3D images for automatic objective assessment of deformable image registration accuracy

Guillaume Cazoulat[1], Brian M. Anderson[1], Molly M. McCulloch[1], Dalia Elganainy[2], Mohamed Zaid[2], Peter C. Park[2], Eugene J. Koay[2], and Kristy K. Brock[1]
1 Department of Imaging Physics, The University of Texas MD Anderson Cancer Center
2 Department of Radiation Therapy, The University of Texas MD Anderson Cancer Center

JULY 12–16 2020 VIRTUAL
JOINT AAPM | COMP MEETING
EASTERN TIME [GMT-4]

INTRODUCTION

Objective assessment of Deformable Image Registration (DIR) often relies on ground truth anatomical displacements established by manual identification of anatomical landmarks in the images.

However, manually (or semi-automatically) picking such landmarks is a process known to be extremely time expensive and is generally reserved for the characterization of DIR uncertainties on small datasets.

While DIR solutions are nowadays available in most treatment planning systems, there is still a need for tools to automatically assess DIR accuracy and detect possible failure.

AIM

In many anatomical localizations, easily identifiable anatomical features correspond to vessel bifurcations which can be detected using image processing techniques. The goal of this study was to propose a workflow to automatically detect corresponding vessel bifurcations in pairs of lung or liver CT scans and to assess their use for the computation of Target Registration Errors (TRE).

MATERIALS AND METHODS

Two datasets were retrospectively analyzed:
- **10 pairs of inhale/exhale phases from lung 4DCTs**, with 300 corresponding landmarks available for each case (DIR-Lab dataset [1,2]).
- **10 pairs of pre/post-radiotherapy liver contrast-enhanced CT scans**, each with 5 manually picked vessel bifurcation correspondences [4].

The workflow proposed to detect landmark correspondences in the pairs of images is detailed in figure 1:
- In all images, the lungs or liver were segmented using the MBS method in RayStation (RaySearch Laboratories) or a deep learning method [3] for the lungs and liver, respectively.
- Using these segmentations as masks, an automatic segmentation of the internal vasculature was performed by computing and thresholding a vesselness image as previously described in [4] and [5].
- Images of the vasculature centerline were computed and bifurcations were detected based on the number of neighbors of each centerline voxel.
- In parallel, the vasculature segmentations were independently registered using a Demons algorithm between representations of their surface with distance maps [5].
- Detected bifurcations were considered as corresponding when distant by less than 4mm after vessels DIR.
- All pairs of images were registered considering a rigid, Anaconda in RayStation and a Demons algorithm.
- Two evaluations of the TRE were performed:
  - **Evaluation A:** the mean TRE was computed using all detected correspondences and compared to the TRE calculated using the available ground truth landmarks correspondences.
  - **Evaluation B:** only the landmarks the closest to the ground truth landmarks where used for TRE calculation.

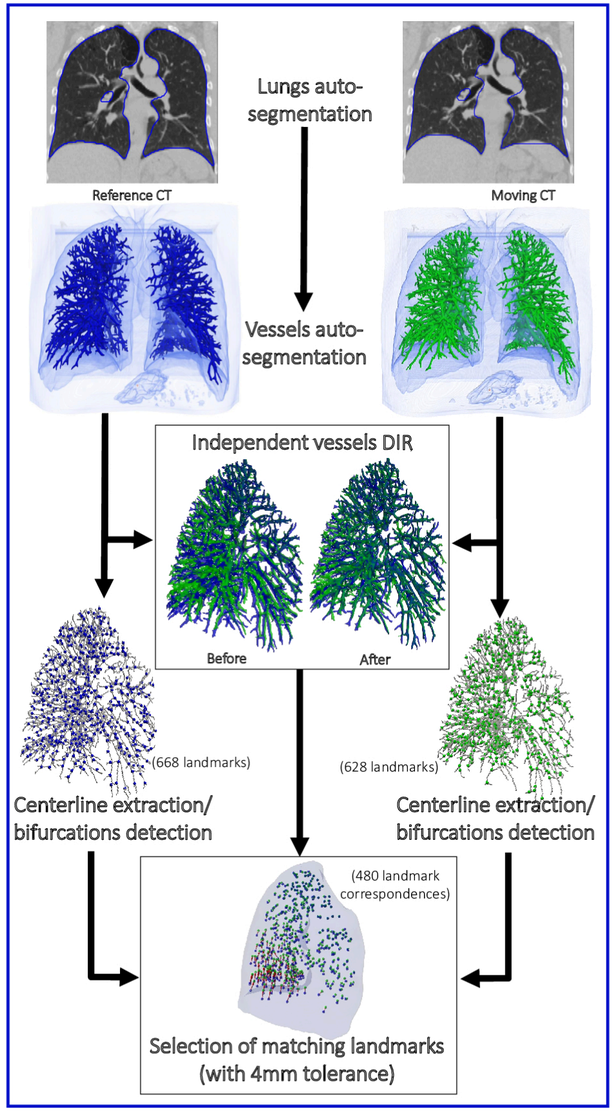

Figure 1. Workflow of the automatic definition of landmarks for TRE calculation. Example with a lung case from the DIRLab dataset (Case2).

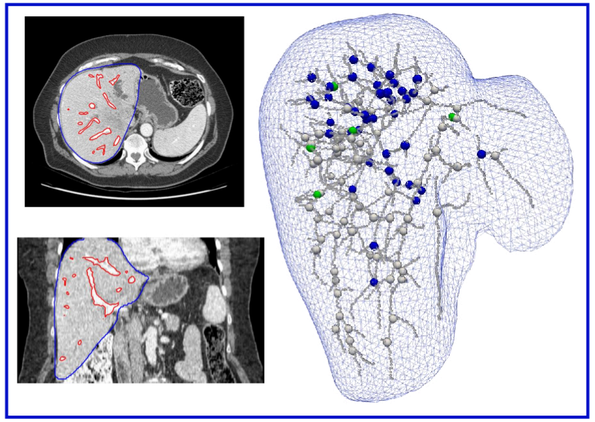

Figure 2. Example of liver case. Left images: axial and coronal slices of the pre-treatment contrast enhanced CT scan with the auto-segmentations of the liver (in blue) and vasculature (in red). Right: Representation of the the liver surface and segmented vasculature centerline. Green spheres: the 5 ground truth landmarks. Blue spheres: the detected landmarks for which a correspondence was established on the post-treatment image. White spheres: the bifurcations that were detected in the pre-treatment image but discarded because no reliable correspondence could be established in the post-treatment image according to the vessels DIR.

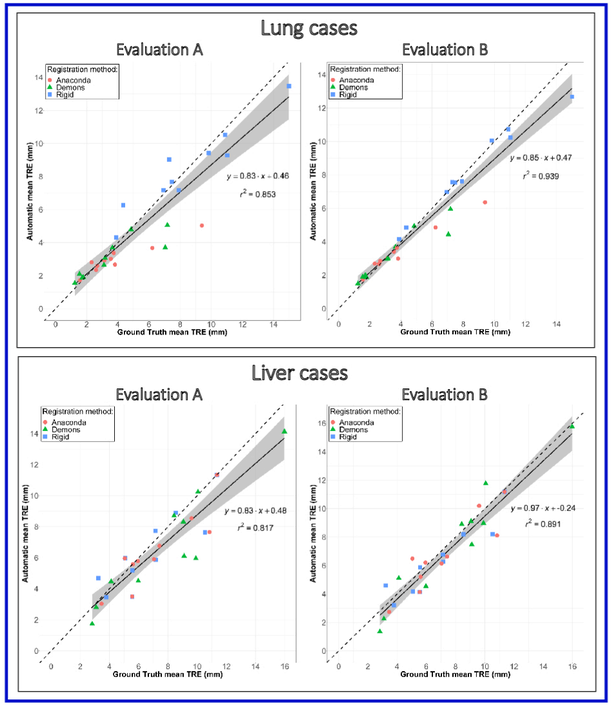

Figure 3. Representation of the correlation between the TREs calculated using the ground truth or automatically detected landmark correspondences. Top row: for the 10 lung cases and 3 registration methods. Bottom row: for the 10 liver cases and 3 registration methods. Left (Evaluation A): TREs calculated using all the detected landmarks. Right (Evaluation B): TREs calculated using only the detected landmarks the closest to the ground truth.

RESULTS

Figure 2 shows an example of bifurcations detection for a liver case. Because of the challenge in visually identifying corresponding bifurcations in this case, the spatial distribution of the manually picked landmarks (green spheres) did not cover a part of the liver as large as the automatically detected bifurcations did (blue spheres). For this reason, differences in mean TRE using either the ground truth or all automatically detected bifurcations, in Evaluation A, could be observed. Evaluation B aimed at validating the proposed automatic approach by comparing the TREs when considering only the landmarks detected the closest to the ground truth landmarks.

Figure 3 shows a strong correlation was obtained between the mean TREs calculated using either the reference or closest detected landmarks (Evaluation B): 0.94 for the lungs dataset and 0.89 for the liver dataset. This correlation was lower when using all the detected landmarks but remained high (Evaluation A): 0.82 for the liver and 0.85 for the lungs, which was likely due to the fact the proposed approach did not constrain the density of detected bifurcations; or in the case of the liver dataset, may have provided a better coverage of the whole liver volume.

CONCLUSION

For lungs or liver CT scans DIR, a strong correlation was obtained between TRE calculated using manually picked or landmarks automatically detected with the proposed method. This tool should be particularly useful in studies requiring to efficiently assess the reliability of a large number of registrations.

REFERENCES

[1] Castillo R, Castillo E, Guerra R, Johnson VE, McPhail T, Garg AK, Guerrero T. 2009. A framework for evaluation of deformable image registration spatial accuracy using large landmark point sets. Phys Med Biol 54 1849-1870.

[2] Castillo E, Castillo R, Martinez J, Shenoy M, Guerrero T. 2009. Four-dimensional deformable image registration using trajectory modeling. Phys Med Biol 55 305-327.

[3] Anderson B, Lin E, Cardenas C, Gress D, Erwin W, Odisio B, Koay E, Brock K. Automated Contouring of Contrast and Noncontrast Computed Tomography Liver Images With Fully Convolutional Networks, Adv Radiat Oncol 2020

[4] Cazoulat G, Owen D, Matuszak MM, Balter JM, Brock KK. Biomechanical deformable image registration of longitudinal lung CT images using vessel information. Phys Med Biol. 2016;61(13):4826-4839.

[5] Cazoulat G, Elganainy D, Anderson BM, Zaid M, Park PC, Koay EJ, Brock KK. Vasculature-Driven Biomechanical Deformable Image Registration of Longitudinal Liver Cholangiocarcinoma Computed Tomographic Scans. Adv Radiat Oncol. 2019 Oct 17;5(2):269-278.

ACKNOWLEDGEMENTS

Research reported was supported in part by the Helen Black Image Guided Fund, in part by the NIH (1R01CA221971-01A1), in part by resources of the Image Guided Cancer Therapy Research Program from The University of Texas MD Anderson Cancer Center, and in part by RaySearch Laboratories AB and University of Texas MD Anderson Cancer Center through a Co-Development and Collaboration Agreement,. Dr Eugene Koay was supported by the Andrew Sabin Family Fellowship, Sheikh Ahmed Center for Pancreatic Cancer Research, Khalifa Foundation, equipment support by GE Healthcare and the Center of Advanced Biomedical Imaging, and NIH (U54CA210181.01, U54CA143837 and U01CA196403). The work was also supported by the Cancer Center Support Grant (CA016672) to MD Anderson.